Preliminary Steps Towards a Low Power Integrated Circuit for AgriTech: a Relaxation Oscillator for Stem Impedance Monitoring

Mattia Barezzi*, Stefano Calvo*, Luca Rolle*, Danilo Demarchi*, and Umberto Garlando*
*Department of Electronics and Telecommunications, Politecnico di Torino, Torino, Italy

Email: umberto.garlando@polito.it

***Abstract*—The main challenges in modern agriculture involve addressing the disruptive environmental effects caused by crop and livestock production, which are essential for human survival. Emerging trends point towards a world of pervasive IoT (Internet of Things) nodes, where low-cost, low-power, and in-vivo plant sensors can detect abiotic and biotic stresses at the earliest stages. This paper presents a preliminary study of an integrable, low-power relaxation oscillator, consisting of a Schmitt trigger in a feedback loop with the plant's stem to evaluate its health status. Simulations have been conducted to compare the energy consumption of this circuit with state-of-the-art electronic sensors, focusing on energy usage per measurement. The results indicate that this new solution can sense the plant's health status with an energy consumption below 10 µJ per measurement, which is at least an order of magnitude lower than existing electronic systems found in the literature.**

***Index Terms*—Impedance Monitoring, Microelectronics, In-vivo Monitoring, Smart Agriculture, Sustainable Agriculture**

I. Introduction

Agriculture significantly impacts the environment, contributing to climate change and pollution [1]. Sustainable agriculture balances food production with soil health preservation. Sensors optimize yield and resource conservation. They monitor abiotic and biotic stresses affecting plants. In particular, low-cost, low-power sensors enable real-time stress detection, improving sustainability. There are three noteworthy research-grade, low-cost, low-power solutions for detecting plant health. These sensors allow for the observation of the plant's interior, enabling the early detection of water or nutrient abiotic stress before visible symptoms appear, as well as biotic stress from pests or pathogens before they spread across the field. The first is the use of an Organic Electrochemical Transistor (OECT) [2], called bioristor, to sense ion concentration in plant sap, with a dedicated circuit to convert changes in OECT conductance into a measurable voltage. The second involves performing Electrical Impedance Spectroscopy (EIS) along a frequency range or an Impedance Measurement (IM) at a specific frequency applied to a part of the plant [3]. For instance, commercial integrated circuits such as the AD5933 (Analog Devices, Wilmington, USA) can be used, as demonstrated in [4], where this technique is applied directly to fruit ripening stage evaluation. This concept can be extended to plant water stress monitoring by placing two electrodes into the plant stem and perform an EIS [5] or by measuring stem electrical impedance at a particular frequency [6]. Lastly, there is the approach of using a relaxation oscillator in feedback with the plant itself: the generated square-wave frequency is inversely correlated to the modulus of the stem's impedance, as demonstrated in [7]. This method utilizes a LMC555 (Texas Instruments, Dallas, USA) integrated circuit: a 555 timer in a relaxation oscillator configuration, oscillating at tens of kHz where a relative variation of -15% has been observed from healthy to water stress condition in a *Nicotiana Tabacum* cultivar during the experimental period [7]. This latter solution is ideal for integration since it does not require complex reading analog circuits but only a digital element, such as a timer, to estimate the oscillating frequency generated by the relaxation oscillator. In addition, its low power consumption enables the use of battery-powered devices with multi-year lifespans or energy-autonomous systems without the need for batteries [8], [9], ensuring long-term operation and minimal maintenance. However, the commercial integrated circuit used for this sensor is not specifically designed for this task but it is intended to be as versatile as possible. Consequently, this paper proposes a preliminary study on a low-cost and low-power Schmitt Trigger (ST) in a relaxation oscillator configuration for direct plant monitoring in climate-smart agriculture applications.

This work was funded under the National Recovery and Resilience Plan (NRRP), Mission 4 - Component 2 - Investment 3.1 - Call for tender No. n. 3264 of 28/12/2021 of Italian Ministry of Research funded by the European Union – NextGenerationEU - Project code: IR0000027, Concession Decree No. 128 of 21/06/2022 adopted by the Italian Ministry of Research, CUP: B33C22000710006, Project title: iENTRANCE, and within the Agritech National Research Center receiving funding from the European Union Next-GenerationEU (PIANO NAZIONALE DI RIPRESA E RESILIENZA (PNRR) – MISSIONE 4 COMPONENTE 2, INVESTIMENTO 1.4 – D.D. 1032 17/06/2022, CN00000022). This manuscript reflects only the authors' views and opinions, neither the European Union nor the European Commission can be considered responsible for them.

II. Proposed Design

The main component of the proposed Relaxation Oscillator (RO) is the ST. This element is a comparator circuit with hysteresis, where an analog input signal is converted into a digital output signal. The Schmitt trigger is typically used in signal conditioning applications to remove noise from signals in digital circuits, but it can also be configured in a closed-

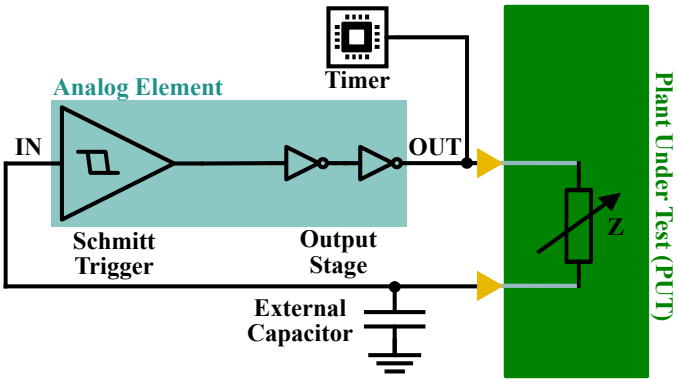

Fig. 1. Relaxation oscillator scheme in a climate-smart agriculture application.

loop feedback system to implement a relaxation oscillator: a nonlinear electronic oscillator that produces a square wave signal. When external load-driving capability is required, an output stage (such as an inverter chain) is added at the output of the Schmitt trigger. A startup circuit to initiate oscillation is not needed in a similar way as in a ring oscillator: an odd number of inverting stages, in the proposed design composed of an inverting Schmitt trigger and two inverters, allows for a net phase shift equal to 180°. This configuration is referred to as the "Analog Element," (AE) as shown in Fig. 1.

Fig. 1 illustrates a potential application of this design in a smart agriculture scenario. Consider placing two bio-compatible electrodes [7] in the stem of a plant, referred to as the Plant Under Test (PUT). Between the two electrodes, an unknown plant stem electrical impedance (Z) is present. One electrode (the yellow triangle in Fig. 1) is connected to the input (IN) of the Analog Element, with an external capacitor connected in parallel. The output (OUT) of the Analog Element is connected to the other electrode inserted in the plant's stem. When a supply voltage is provided the output switches between logic '0' and logic '1'. This results in the charging and discharging of the external capacitor following an exponential curve. Since the output OUT signal is digital (so, V_{dd} or 0 V), the output is a square wave. This signal frequency can be measured by a timer (or a microcontroller with a timer peripheral) and it is inversely correlated to the stem impedance modulus $|Z|$ at the oscillating frequency [7], [9]. The Analog Element was implemented using a ST in the Dokić topology [10]. This topology uses six MOS (Metal Oxide Semiconductor) transistors, three PMOS and three NMOS, to achieve an adjustable hysteresis window and the typical Schmitt trigger input-output characteristic. Additionally, an output stage consisting of two inverters is included to drive external loads, such as the external capacitor, and the unknown stem electrical impedance modulus ($|Z|$) of the PUT. The time constant in charging and discharging the external capacitor determines the oscillation frequency. Fig. 2 shows the transistor-level topology of the Analog Element. Transistors M1, M2 and M3 set the upper switching point where, instead M4, M5, M6 set the lower switching point. This approach is based on the detailed description provided in [11]. Finally, M7, M8 and M9, M10 compose, respectively, the first and second inverter to driving external loads.

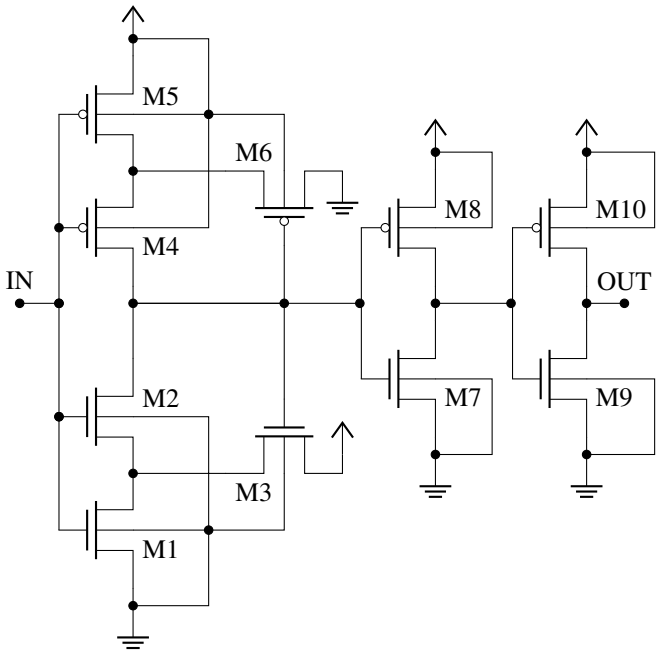

Fig. 2. Transistor-level topology of the Analog Element.

V_{dd} is set to 1.8 V, which is a typical commercial supply voltage. V_{spl} and V_{sph}, respectively the lower and upper switching points, are chosen as 0.6 V and 1.2 V setting the time of the charging and discharging phases of the external capacitor. These switching points are chosen to allow for a fair comparison with respect to the LMC555 supplied at 1.8 V, as in [7]. The external capacitor is typically in the nF range, ensuring oscillation frequencies in the tens of kHz with typical plant impedance modulus values as for example, *Nicotiana Tabacum* plants, ranging from tens of kΩ and hundreds of kΩ [6] in, respectively, healthy and heavy drought conditions.

This topology allows for the lower and upper switching points to be determined based on the ratio of transistor dimensions as defined in Eq. (1).

$$\begin{aligned} \frac{W_1 L_3}{L_1 W_3} &= \left(\frac{V_{dd}-V_{sph}}{V_{sph}-V_{thn}}\right)^2 \\ \frac{W_5 L_6}{L_5 W_6} &= \left(\frac{V_{spl}}{V_{dd}-V_{spl}-V_{thp}}\right)^2 \end{aligned} \tag{1}$$

where each transistor M_x has its W_x, width of the MOS, and L_x, length of the MOS. V_{thn} and V_{thp} are, respectively, the threshold voltages of the NMOS and the PMOS.

Transistors M2 and M4 are used as switches. Moreover, their size ratios must be equal to or greater than those of the MOS transistors used for setting the upper and lower thresholds. Table I lists the key parameters used in the Analog Element. Table II shows the geometrical values used in the design of the Analog Element for each transistor. L_x in Table II indicates that all MOS transistors in the ST have equal length.

TABLE I
MAIN PARAMETERS USED IN THE ANALOG ELEMENT

Variable	V_{dd}	V_{spl}	V_{sph}	V_{thn}	V_{thp}
Value	1.8 V	0.6 V	1.2 V	0.71 V	−0.73 V

TABLE II
GEOMETRICAL VALUES USED IN THE ANALOG ELEMENT

Variable	**Value**
L_x	1 µm
W_1, W_2	1.5 µm
W_3, W_6, W_7	1 µm
W_4, W_5	1.63 µm
W_8	2 µm
W_9	10 µm
W_{10}	20 µm

The period of the discharging and charging oscillation time, respectively t_1 and t_2, are calculated using the Eq. (2).

$$\begin{aligned} t_1 &= R_{plant} \cdot C_{ext} \cdot \ln\left(\frac{V_{sph}}{V_{spl}}\right) \\ t_2 &= R_{plant} \cdot C_{ext} \cdot \ln\left(\frac{V_{dd}-V_{spl}}{V_{dd}-V_{sph}}\right) \end{aligned} \quad (2)$$

where C_{ext} is the external capacitance used and R_{plant} is the equivalent resistance of the stem track of the plant. In the real scenario, a complex impedance Z is present in the stem track of the plant. In this preliminary study, it is important the determination of a realistic impedance modulus range to perform the simulations of the relaxation oscillator in the desired frequency range (between 10 kHz and 100 kHz). The idea is not to determine a precise relation between the stem electrical impedance modulus and the resulting oscillating frequency, but to find a range where the sensitivity, evaluated as the oscillating frequency variations over time, is maximised. Therefore, the goal is to exploit the relative oscillating frequency variation over time to detect abiotic and biotic stresses in the plant. Thus, the oscillation period t_{osc} is as in Eq. (3).

$$t_{osc} = t_1 + t_2 \quad (3)$$

Since by design $t_1 = t_2$, the resulting signal will be a 50% duty cycle square wave. Substituting the values from Table I, we obtain as in Eq. (4).

$$t_{osc} = 1.386 \cdot R_{plant} \cdot C_{ext} \quad (4)$$

III. RESULTS AND DISCUSSIONS

The designed low-complexity low-power RO needs to be analysed in terms of relative error with respect to the theoretical computation shown in Section II and required energy for single measurement. A layout was designed using the Cadence Virtuoso environment in TSMC180 technology, resulting in a design of 38.13 µm by 17.72 µm, giving a total area footprint of approximately 676 µm^2. Fig. 3 shows the layout used for post-layout simulations. Most of this area is due to the output

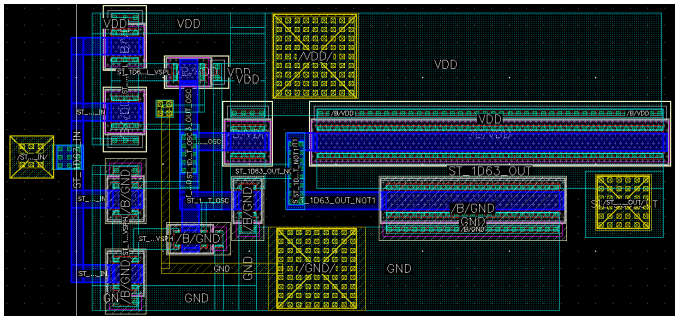

Fig. 3. Layout of the Analog Element.

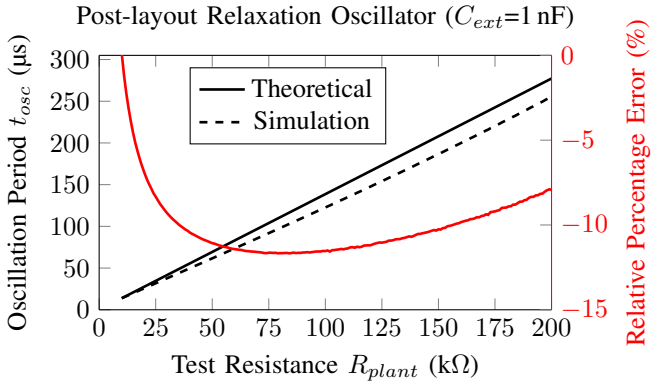

Fig. 4. Oscillation period against test resistance curve considering the simulated relaxation oscillator with C_{ext}=1 nF.

stage, composed of two inverter stages, which are necessary to drive external load capacitances and resistances, such as, for example, the pins of external chips, a microcontroller, or a timer. The sizes of the output stage could be adjusted in future designs according to the driving capability requirements.

A testbench of the relaxation oscillator was implemented, considering a load capacitance and a load resistance between a node (IN and OUT) and ground. Their values are 50 pF

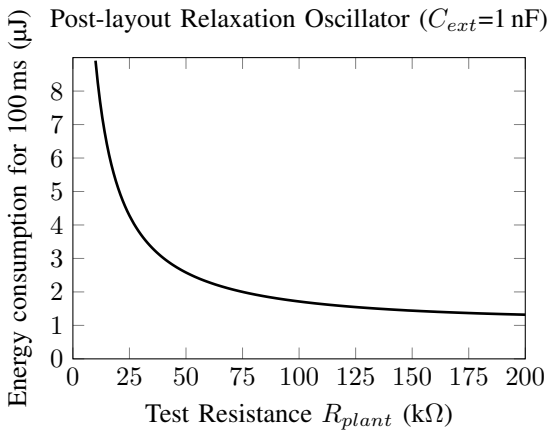

Fig. 5. Energy drawn for a single measurement lasting 100 ms against test resistance curve considering the simulated relaxation oscillator with C_{ext}=1 nF.

TABLE III
ENERGY CONSUMPTION FOR SINGLE MEASUREMENT

Method	Note	Avg. Curr/Power	Meas. Time	Energy per Meas.	Reference
CE with Bioristor	Large contrib. are c.c. and ADC reported in [12]	2.3 mA	N.A.	N.A.	[12]
IM with AD5933	/	50.0 mW	3 ms	150.0 µJ	[13]
EIS with AD5933	/	50.0 mW	>3 ms	>150.0 µJ	[13]
FE with LMC555	Exp. meas. based on system in [9] @1.8 V	532.8 µW÷714.6 µW	100 ms	53.3 µJ÷71.5 µJ	This work
FE with Schmitt trigger	Post-layout simulations @27 °C@1.8 V	13.2 µW÷89.1 µW	100 ms	1.3 µJ÷8.9 µJ	This work

and 1 MΩ, respectively, and they are compatible with the typical values of external chips. The relaxation oscillator requires an external capacitance (referred to as C_{ext}). The frequency range considered for *Nicotiana Tabacum* is between 10 kHz and 100 kHz. These frequencies were selected based on the noisy behavior of stem impedance below this range [5] and to improve sensitivity, based on new experiments on *Nicotiana Tabacum*. The selected boundaries identify a good working range and an effective trade-off between low noise and energy consumption per single measurement. These choices contribute to the low-cost aspect: such low frequencies are compatible with larger technology nodes (180 nm), which are cheaper compared to more advanced ones. As described in Section II, to emulate the impedance modulus $|Z|$ range in the plant, a simple set of resistances could be considered. More advanced models of plant stems could be used, but for this preliminary study, a simpler model was selected. A possible range of resistances modeling a plant stem is from 10 kΩ to 200 kΩ [6]. Finally, for the good sensitivity range, we could consider a capacitance equal to 1 nF. Moreover, replacing a complex model of the plant stem with a resistor (referred to as Test Resistance R_{plant}) could help to focus on the development of the relaxation oscillator. Fig. 4 shows the relationship between the considered test resistance expressed in kΩ and the resulting oscillating period of the square wave signal OUT in microseconds. A comparison between the theoretical value described in Section II and the post-layout simulated value indicates a limited relative percentage error of less than 12% in all considered test resistance cases. For this preliminary study, this error can be considered acceptable. More interesting is the analysis of the energy consumption of the simulated AE. First, the energy consumption was extracted in the most realistic case with respect to the state-of-the-art literature. Fig. 5 illustrates the energy consumption for 100 ms of oscillation at a frequency depending on the considered test resistance. A measurement period of 100 ms is reasonable (the period to supply the relaxation oscillator). Tests on *Nicotiana Tabacum* were conducted using the relaxation oscillator configured with the LMC555, as described in [9]. A lower value results in considerable errors due to a non-negligible start-up time required to charge all parasitic capacitances in the plant, as well as the need for a minimum number of samples to compute a simple average of the obtained readings. Conversely, a higher value would lead to unnecessary energy waste, reducing the electronic system's lifetime. To appreciate the energy impact, Table III shows the energy measurements for a single measurement on the plant compared to the methods presented in Section I.

In particular, the Conductance Evaluation (CE) in the bioristor requires a conditioning circuit to bias the OECT and an active ADC to sample the voltage. The authors in [12] report an average of 2.3 mA for the sensor reading measurement time over an unspecified period; moreover, an energy per measurement evaluation is not possible. Regarding Impedance Measurement (IM) using AD5933, [13] reports approximately 150 µJ for impedance modulus and phase for a single frequency. Electrical Impedance Spectroscopy (EIS) is possible with the same chip, gathering more than one valuable frequency at the cost of greater energy consumption.

Frequency Evaluation (FE) of a relaxation oscillator based on the LMC555 circuit as described in [9] was analyzed, and an experimental campaign of power consumption was performed at the same supply voltage used in the simulations (1.8 V), estimating the resulting frequency. The result shows that the energy consumption for 100 ms is equal to 53.3 µJ÷71.5 µJ, generating an oscillating frequency range of 22.7 kHz÷196.0 kHz using a set of test resistances on LMC555 system ranging from 1 kΩ to the open circuit condition (no resistance connected). The power contributions arise from the presence of biasing currents for comparators, latch set-reset, and the resistor divider network. These elements could be avoided in the realization of a simple Schmitt trigger. Finally, simulations obtained using the proposed relaxation oscillator, considering a temperature of 27 °C and a voltage of 1.8 V, yielded a range of 13.2 µW÷89.1 µW. Thus, for a 100 ms measurement, an energy draw of 1.3 µJ÷8.9 µJ was observed.

IV. CONCLUSIONS

A preliminary study on a low-power relaxation oscillator for stem impedance monitoring was conducted. The proposed system was compared to research-grade sensors from state-of-the-art literature on climate-smart agriculture, aiming to directly evaluate plant health in-vivo. The electronic system consumed less than 10 µJ per measurement, a significantly lower amount than other systems. This efficiency is crucial for precision agriculture, reducing maintenance and costs. As a next step, an analysis of PVT (Process, Voltage, Temperature) variations should be completed before prototype chip production. Process variations, temperature coefficients, and line sensitivity may be compensated using external digital-based circuitry.

REFERENCES

[1] Food and Agriculture Organization of the United Nations, *The State of the World's Land and Water Resources for Food and Agriculture 2021 – Systems at breaking point*. FAO, May 2022. [Online]. Available: http://dx.doi.org/10.4060/cb9910en

[2] N. Coppedè, M. Janni, M. Bettelli, C. L. Maida, F. Gentile, M. Villani, R. Ruotolo, S. Iannotta, N. Marmiroli, M. Marmiroli *et al.*, "An in vivo biosensing, biomimetic electrochemical transistor with applications in plant science and precision farming," *Scientific reports*, vol. 7, no. 1, p. 16195, 2017.

[3] I. Jócsák, G. Végvári, and E. Vozáry, "Electrical impedance measurement on plants: a review with some insights to other fields," *Theoretical and Experimental Plant Physiology*, vol. 31, no. 3, pp. 359–375, 2019.

[4] P. Ibba, M. Crepaldi, G. Cantarella, G. Zini, A. Barcellona, M. Rivola, M. Petrelli, L. Petti, and P. Lugli, "Design and validation of a portable ad5933–based impedance analyzer for smart agriculture," *IEEE Access*, vol. 9, pp. 63 656–63 675, 2021.

[5] U. Garlando, L. Bar-On, P. M. Ros, A. Sanginario, S. Calvo, M. Martina, A. Avni, Y. Shacham-Diamand, and D. Demarchi, "Analysis of in vivo plant stem impedance variations in relation with external conditions daily cycle," in *2021 IEEE International Symposium on Circuits and Systems (ISCAS)*. IEEE, 2021, pp. 1–5.

[6] U. Garlando, S. Calvo, M. Barezzi, A. Sanginario, P. M. Ros, and D. Demarchi, "Ask the plants directly: Understanding plant needs using electrical impedance measurements," *Computers and Electronics in Agriculture*, vol. 193, p. 106707, 2022.

[7] U. Garlando, S. Calvo, M. Barezzi, A. Sanginario, P. M. Ros, and D. Demarchi, "A "plant-wearable system" for its health monitoring by intra- and interplant communication," *IEEE Transactions on AgriFood Electronics*, vol. 1, no. 2, pp. 60–70, 2023.

[8] S. Calvo, M. Barezzi, U. Garlando, R. La Rosa, and D. Demarchi, "An energy autonomous and battery-free plant's electrical impedance measurement system," in *2024 IEEE International Symposium on Circuits and Systems (ISCAS)*, 2024, pp. 1–4.

[9] S. Calvo, M. Barezzi, D. Demarchi, and U. Garlando, "In-vivo proximal monitoring system for plant water stress and biological activity based on stem electrical impedance," in *2023 9th International Workshop on Advances in Sensors and Interfaces (IWASI)*. IEEE, 2023, pp. 80–85.

[10] B. Dokić, "Cmos schmitt triggers," *IEE Proceedings G (Electronic Circuits and Systems)*, vol. 131, pp. 197–202(5), October 1984. [Online]. Available: https://digital-library.theiet.org/content/journals/10.1049/ip-g-1.1984.0037

[11] R. J. Baker, *CMOS Circuit Design, Layout, and Simulation*, 3rd ed. Wiley-IEEE Press, 2010.

[12] A. Boni, E. Graiani, V. Bianchi, I. De Munari, and M. Caselli, "A wireless biosensor node for real-time crop monitoring in precision agriculture," in *2024 IEEE International Symposium on Circuits and Systems (ISCAS)*, 2024, pp. 1–5.

[13] G. Laput, R. Xiao, X. A. Chen, S. E. Hudson, and C. Harrison, "Skin buttons: cheap, small, low-powered and clickable fixed-icon laser projectors," in *Proceedings of the 27th Annual ACM Symposium on User Interface Software and Technology*, ser. UIST '14. New York, NY, USA: Association for Computing Machinery, 2014, p. 389–394. [Online]. Available: https://doi.org/10.1145/2642918.2647356